

# High temperature of laser-compressed shells measured with $\text{Kr}^{34+}$ and $\text{Kr}^{35+}$ x-ray lines

B. Yaakobi, F. J. Marshall, and R. Epstein

Laboratory for Laser Energetics, University of Rochester, 250 East River Road, Rochester, New York 14623-1299

(Received 4 June 1996)

High electron temperatures (3–4 keV) have been achieved by imploding shells filled with a deuterium-krypton mixture on the OMEGA laser system, in agreement with hydrodynamic simulations. The temperature was deduced from the high-energy continuum slope in the range 8–20 keV, and from the intensity ratio of  $\text{Kr}^{35+}$  to  $\text{Kr}^{34+}$  x-ray lines. These results show the feasibility of obtaining higher temperatures than previously achieved in laser implosions and studying them using spectroscopy of sub-Å x-ray lines and continuum. [S1063-651X(96)06611-1]

PACS number(s): 52.50.Jm

The achievement of high temperatures with laser-imploded targets is of interest for studying the physics of laser fusion and other plasmas. Simulations [1] show that high electron temperatures of up to 5 keV should be achieved with laser systems such as the OMEGA system at the Laboratory for Laser Energetics [2] using relatively thin-shell targets. These temperatures should occur at modest compression densities ( $\sim 1\text{--}5\text{ g/cm}^3$ ), and the ion temperature should peak above 10 keV. These simulations also show that the addition of a small amount of krypton gas ( $\sim 0.03$  atm) to the hydrogenic fuel should produce strong emission of  $\text{Kr}^{35+}$  and  $\text{Kr}^{34+}$  x-ray lines, while reducing the compressed-fuel temperature by only a negligible amount. We report on a series of experiments in which these predictions have been demonstrated: high electron temperatures (3–4 keV) were indeed measured using intense heliumlike and hydrogenlike krypton lines as well as high-energy continuum. High ion temperatures ( $\sim 13$  keV) were likewise deduced from the energy spectrum of the neutrons produced by the deuterium-deuterium (DD) reaction and reported earlier [3].

Results from the present experiments are shown from two target shots for which the experimental parameters are listed in Table I. The shells in these experiments were of CH polymer and the laser pulse had a Gaussian shape of 0.6 ns full width at half maximum. In the first shot, a Si(111) diffracting crystal was used, tuned to detect the spectral range 7–13 keV, while in the second shot a LiF(200) crystal was used, tuned to the range 12–20 keV. Figures 1 and 2 show a comparison between the measured and simulated spectra from the two Kr-doped target shots listed in Table I. Figures 1(a) and 2(a) show the uncalibrated experimental spectrum in film density units. Figures 1(b) and 2(b) show the time- and space-integrated simulations of the same spectra, by the hydrodynamic code LILAC [4]. The unit (keV/keV) refers to

radiation energy per unit of photon energy. The simulated spectrum is plotted on a linear scale, in line with the fact that film density and exposure are approximately linear for these photon energies (see below). Instrumental broadening of the lines has been included in the simulation. The wavelengths of the krypton lines marked in Figs. 1 and 2 are known from the literature [5]. The He- $\alpha$  line ( $1s2p\ ^1P_1\text{--}1s^2\ ^1S_0$ ) is accompanied by lithiumlike and berylliumlike dielectronic satellites on its lower-energy side, which are barely resolved in Fig. 1(a); a high-resolution spectrum of this group of lines was obtained using an electron beam ion trap facility [6].

TABLE I. Experimental parameters of the two target shots used in the krypton spectra analysis.

Shot no.	Target diameter ( $\mu\text{m}$ )	Target thickness ( $\mu\text{m}$ )	DD pressure (atm)	Krypton pressure (atm)	Laser energy (kJ)
4952	870	10	10	0.03	23.6
5110	874	12.4	10	0.03	29.5

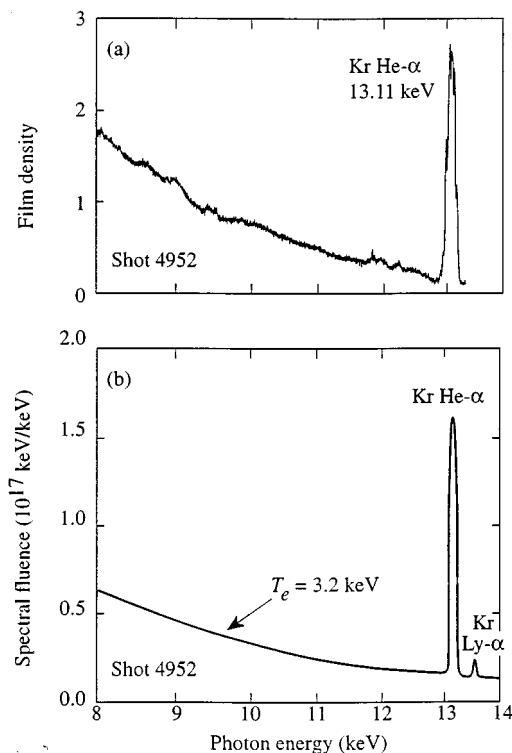


FIG. 1. (a) Experimental spectrum from Kr-doped, DD-filled target shot 4952; (b) LILAC simulation of the same spectrum. The unit (keV/keV) refers to radiation energy per unit of photon energy. The continuum slope in the range of 8–12 keV implies an electron temperature of  $T_e = 3.2$  keV. Instrumental broadening of the calculated lines has been included. The simulation does not include the satellite lines on the low-energy side of the He- $\alpha$  line.

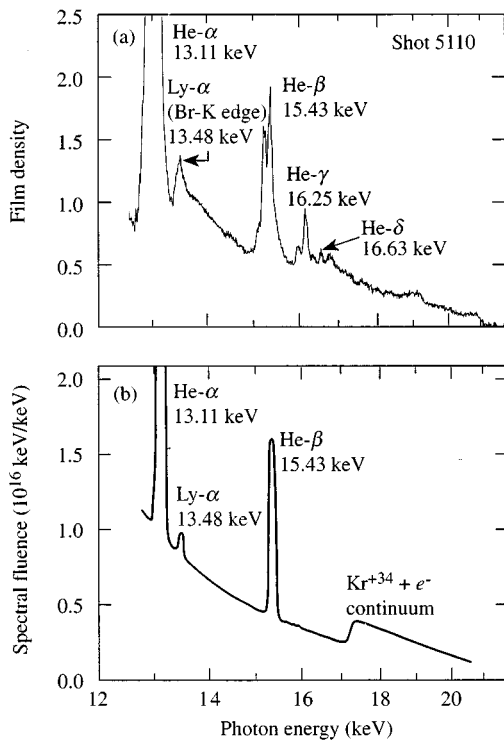


FIG. 2. (a) Experimental spectrum from Kr-doped, DD-filled target shot 5011. The He- $\alpha$  line has a film density  $>5$  and it saturates the film. The continuum slope in the range 16.5–20.5 keV implies an electron temperature of 4.0 keV. (b) LILAC simulation of the same spectrum. The unit (keV/keV) refers to radiation energy per unit of photon energy. The simulation does not include the satellite lines on the low-energy side of the He- $\beta$  line nor the lines above 16 keV. Instrumental broadening of the calculated lines has been included.

The He- $\alpha$  line in Fig. 2(a) has a film density higher than five and it saturates the film. In comparing the measured and simulated spectra, it should be noted that LILAC does not calculate the satellite lines on the low-energy side of the He- $\alpha$  and He- $\beta$  lines, nor the lines above 16 keV. These latter lines cause the apparent continuum jump (due to recombination of Kr<sup>34+</sup> ions) to move from  $\sim 17$  keV in the simulation to  $\sim 16$  keV in the experiment.

To quantitatively analyze the spectra, the response of the film (Kodak DEF) and the crystals (LiF and Si) have to be known. Henke *et al.* [7] published a model for the response of DEF film and normalized it to experimental values below 10 keV. Using this model and updated x-ray absorption coefficients in the film constituents, we extended the calculated film response to photon energies above 10 keV [3]. The results show that for film densities below  $\sim 2$  D and photon energies above  $\sim 6$  keV, the film density is proportional to exposure. This is the reason for plotting the spectral fluence in Figs. 1 and 2 on a linear scale.

Published diffraction data were used for the Si(111) crystal [8] and the LiF(200) crystal [9,10]. It should be emphasized that for the purpose of temperature determination only the change with photon energy of the film and crystal responses is required. The crystal reflectivities change slowly over the relevant energy ranges: the reflectivity of Si(111) over the range 8–12 keV and that of LiF(200) over the range 16–20 keV changes by less than  $\sim 20\%$ . Using the film ex-

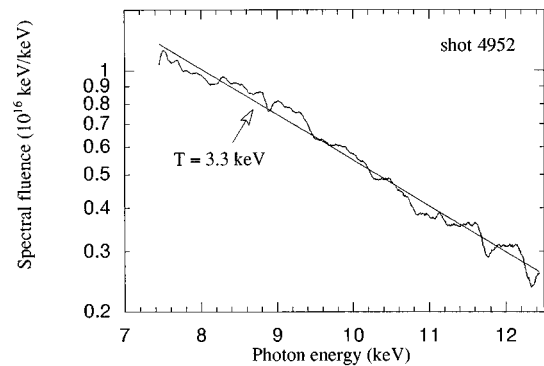


FIG. 3. Experimental continuum spectrum of Fig. 1(a) after absolute calibration. The unit (keV/keV) refers to radiation energy per unit of photon energy. The slope in the range 10–13 keV indicates an electron temperature of  $T_e = 3.3$  keV.

posure  $I(\text{keV}/\text{cm}^2)$  and the integrated crystal reflectivity  $R(E)$ , the spectral fluence per unit solid angle of the target at a photon energy  $E(\text{keV})$  is given by  $S(\text{keV}/\text{keV}) = I(E)L^2 \tan \theta_B / (RE \cos \alpha)$ , where  $E$  is in keV,  $L$  is the target-film distance (along the ray),  $\theta_B$  is the Bragg angle, and  $\alpha$  is the angle of incidence on the film.

Using the film and crystal calibrations as described above, the continuum in the range 7–12 keV (from Fig. 1) and in the range 16.5–20.5 keV (from Fig. 2) were used to estimate the electron temperature. The continuum emission comes mostly from free-free and free-bound emissions due to krypton ions in the compressed core; both processes depend on the photon energy like  $I(E) \sim \exp(-E/kT)$  [11], thus fitting an exponential curve to the calibrated spectrum yields the electron temperature. Figure 3 shows the result for shot 4952 (Fig. 1), where fitting to the continuum yields a temperature of 3.3 keV. This agrees with the simulated temperature of 3.2 keV indicated in Fig. 1(b), using the continuum slope in the range of 8–12 keV. A similar fit to the continuum in the range 16.5–20.5 keV (from Fig. 2) yields a temperature of  $\sim 3.6$  keV. This higher temperature is due mostly to using a higher-energy section of the continuum, which samples higher-temperature target regions and implosion times. The uncertainty in the measured temperature is due mostly to the uncertainty in the relative crystal sensitivity; this is because the film density is very nearly proportional to the intensity and the variation with photon energy is determined by the energy dependence of the x-ray absorption in the film constituents, which is well known [7]. Comparison of various crystal calibrations [9,10,12] shows that the relative sensitivity versus photon energy changes by less than 20% from sample to sample (the absolute sensitivity may change by more than that); this is particularly true in Ref. [10] where five samples of LiF(111) were tested. Using the various calibrations available resulted in temperature variations  $\pm 20\%$ . LILAC results show that the space-averaged temperatures around peak compression in these shots were 3–4 keV and the maximum temperatures were 5–6 keV. The absolute magnitude of the continuum is lower than the simulated spectrum by factors of 3–4. Comparison of the absolute magnitude of spectral lines is complicated by such factors as detailed atomic physics modeling and the spatial distribution of the emitting source. The lower-than-predicted intensity is most likely the result of lower peak temperature and density as compared with the one-dimensional code predictions. This

deviation from predictions is consistent with the lack of beam smoothing on the laser at the time of these experiments.

An additional method for estimating the electron temperature involves the measured intensity ratio of the Lyman- $\alpha$  line of Kr<sup>35+</sup> to the helium- $\beta$  line of Kr<sup>34+</sup>. As described in Ref. [1], this ratio is highly sensitive to the temperature below  $\sim 8$  keV and changes very little with density. Also, the spectral lines chosen can have a relatively low opacity (unlike that of the He- $\alpha$  line); this is true for the krypton fill pressure and compression in these experiments. However, it was shown [13] that a high opacity of the He- $\alpha$  line can indirectly increase the Lyman- $\alpha$  to helium- $\beta$  intensity ratio for the same temperature, because the He- $\alpha$  opacity facilitates ionization of the heliumlike state through  $n=2$  excited Kr<sup>34+</sup> ions. Figure 4 shows curves of the calculated intensity ratio of these two lines [1], with and without a correction for the opacity of the He- $\alpha$  line. The curve used here for the temperature determination corresponds to the estimated opacity ( $\tau \sim 15$ ) for shot 5110. A complication arises because the energy of the  $K$  edge of Br in the film grains (13.475 keV) is very close to the energy of the Lyman- $\alpha$  line of Kr<sup>35+</sup> (13.482 keV). This edge gives rise to a jump in the film sensitivity of almost a factor of 2 [3]; however, the corresponding jump in the measured spectrum should be smaller because of the finite spectral resolution of the spectrometer, which blends the intensity around the jump. To account approximately for this effect, the continuum at energies above the  $K$  edge was extrapolated toward lower energies and the resulting jump in the continuum was subtracted from the measured peak at 13.5 keV. A similar result was obtained when converting film density to exposure and accounting for the finite spectral resolution due to the source size and the crystal resolution. This last method was verified by measuring the spectrum from a target with no krypton. Here, the film density spectrum shows a jump at the Br  $K$  edge, whose slope indicates the effective spectral resolution.

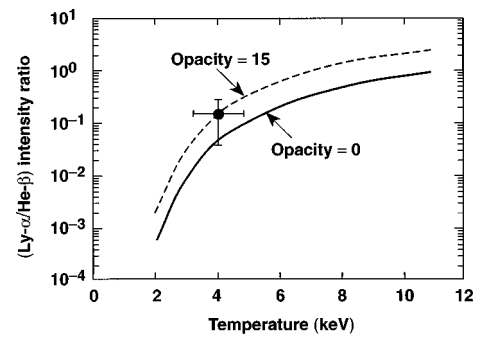


FIG. 4. Electron temperature determination by the measured intensity ratio of the Lyman- $\alpha$  to helium- $\beta$  lines. The curves of calculated intensity ratio are taken from Ref. [13]. This ratio depends weakly on the density but strongly on the opacity of the He- $\alpha$  line. The curve used here for the temperature determination corresponds to the estimated opacity ( $\tau=15$ ) for shot 5110.

The resulting estimated temperature (see Fig. 4) is 4.1 keV. The large uncertainty in the intensity ratio (due mostly to the procedure of determining the intensity of the Lyman- $\alpha$  line) results in only an uncertainty of  $\pm 25\%$  in the temperature; this is similar to the uncertainty in the continuum slope method described above.

In addition to measuring the temperature, krypton lines can also be employed [1] to measure the ion temperature (using a high-spectral-resolution spectrometer) as well as the areal density of the core and core-shell mixing (using a higher krypton pressure). The results reported here indicate the feasibility of such experiments.

This work was supported by the U.S. Department of Energy Office of Inertial Confinement Fusion under Cooperative Agreement No. DE-FC03-92SF19460, the University of Rochester, and the New York State Energy Research and Development Authority.

- 
- [1] B. Yaakobi, R. Epstein, C. F. Hooper, D. A. Haynes, and Q. Su, *J. X-ray Sci. Technol.* **6**, 172 (1996).
- [2] T. R. Boehly, R. S. Craxton, T. H. Hinterman, J. H. Kelly, T. J. Kessler, S. A. Kumpan, S. A. Letzring, R. L. McCrory, S. F. B. Morse, W. Seka, S. Skupsky, J. M. Soures, and C. P. Verdon, *Rev. Sci. Instrum.* **66**, 508 (1995).
- [3] Laboratory for Laser Energetics LLE Review No. 64, National Technical Information Service Document No. DOE/SF/19460-99, 1995 (unpublished), p. 145.
- [4] Laboratory for Laser Energetics Report No. 16, 1973 (unpublished); Laboratory for Laser Energetics Report No. 36, 1976 (unpublished).
- [5] For the He- $\alpha$  line: U. I. Safranova, *Phys. Scr.* **23**, 241 (1981); for the Lyman- $\alpha$  line: G. W. Erickson, *J. Phys. Chem. Ref. Data* **6**, 831 (1977); for the He- $\beta$ ,  $\gamma$ ,  $\delta$  lines: A. M. Ermolaev and M. Jones, *J. Phys. B* **7**, 199 (1974) and Supplement.
- [6] W. Widmann, P. Beiersdorfer, and V. Decaux, Lawrence Livermore National Laboratory Report No. UCRL-JC-118364, National Technical Information Service document No. DE95010264/XAB, 1994 (unpublished).
- [7] B. L. Henke, J. Y. Uejio, G. F. Stone, C. H. Dittmore, and F. G. Fujiwara, *J. Opt. Soc. Am. B* **3**, 1540 (1986).
- [8] G. Brogren and E. Linden, *Ark. Fys.* **22**, 535 (1962).
- [9] K. Toh, T. Ui, and E. Asada, in *Advances in X-Ray Analysis*, edited by C. S. Barrett, P. K. Predecki, and D. E. Leyden (Plenum, New York, 1985), Vol. 28, p. 119.
- [10] A. J. Burek and B. Yaakobi, Final Report to the National Bureau of Standards, National Technical Information Service Document No. DE83015439 1983 (unpublished), Appendix A.
- [11] H. R. Griem, *Plasma Spectroscopy* (McGraw-Hill, New York, 1964), Chap. 8.
- [12] J. V. Gilfrich, D. B. Brown, and P. G. Burkhalter, *Appl. Spectrosc.* **29**, 322 (1975).
- [13] C. J. Keane, B. A. Hammel, D. R. Kania, J. D. Kilkenny, R. W. Lee, A. L. Osterheld, L. J. Suter, R. C. Mancini, C. F. Hooper, and N. D. Delamater, *Phys. Fluids B* **5**, 3328 (1993).